Transfers Orbit Design from Lunar Frozen Orbit to Near Rectilinear Halo Orbit

LIANG Guoliang，YANG Hongwei

（College of Astronautics, Nanjing University of Aeronautics and Astronautics, Nanjing 211106, China）

Abstract：A multi-maneuver approach to transition from Lunar Frozen Orbit (LFO) to a cislunar L2 Near Rectilinear Halo Orbit (NRHO) was developed in this research. LFO was utilized to provide the navigation or communication platform for lunar exploration. They are long-term stable orbits with constant orbital elements on average. Subsets of Halo orbit families, known as NRHO, are orbits that are nearly stable. Due to their important locations in cislunar space, the L2 NRHO are considered as possible launching platforms for deep space or lunar exploration mission. For upcoming cislunar space exploration missions, the low fuel consumption transfer approach between these orbits is very valuable. Utilizing the maximum stretching direction to determine the insertion maneuver, the spacecraft may rapidly approach NRHO. In order to optimize the transfer trajectories, a nonlinear programming problem was developed. The optimization results with different transfer windows in the high-fidelity model were given for the transfer from LFO to NRHO, demonstrating the reliability of the proposed strategy.

Keywords：trajectory design and optimization；Lunar Frozen Orbit；Near Rectilinear Halo Orbit

Highlights：

- The design of transfer trajectory from LFOs to NRHOs was investigated.
- The maximum stretching direction was utilized to make the spacecraft approach NRHO rapidly with little Δv.
- The transfer trajectories were designed in both CR3BP and high-fidelity model, demonstrating the potential for engineering applications providing new mission orbits for future cislunar space missions.

中图分类号：V448.2　　文献标识码：A　　文章编号：2096-9287(2026)02-0151-11

DOI:10.3724/j.issn.2096-9287.2026.20250106

Reference format: LIANG G L，YANG H W. Transfers orbit design from lunar frozen orbit to near rectilinear Halo orbit[J]. Journal of Deep Space Exploration, 2026, 13 (2) : 151-161.

引用格式：梁国梁，杨洪伟. 月球冻结轨道至近直线晕轨道的转移轨道设计方法[J]. 深空探测学报（中英文），2026，13（2）：151-161.

Introduction

Over the past few years, lunar exploration has aroused considerable interest among researchers and engineers[1]. The Artemis mission, carried out by the National Aeronautics and Space Administration (NASA), lights the hope of human to come back to the lunar again[2]. The Chang'E series lunar exploration program of the China National Space Administration has broken through the issue of sampling and return from the far side of the Moon, which further reveals the mysterious veil of the Moon[3]. The Chandrayaan-3 mission carried out by Indian Space Research Organization is the first successful lunar landing mission of India, which has also provided further understanding of the Moon[4]. With the increasing desire of more and more countries for lunar exploration, the investigation of orbital dynamics in the vicinity of the Moon has become more important. The dynamics in the vicinity of the Moon are tangled and complex. The spacecraft in this area will run under the combined force of the Earth and Moon's gravitation. There are some special orbits in this complex dynamical environment. For example, Lunar Frozen Orbit (LFO) and Near Rectilinear Halo Orbit (NRHO). The circumlunar orbits are alternative options for direct lunar exploration and relay communication

Received：2025-09-10　Revised：2026-03-14

Fund program：Supported by the National Natural Science Foundation of China（12372046） and Natural Science Foundation of Jiangsu Province（BK20220130）

mission orbit. NRHO could not only construct the transition bridge between themselves and circumlunar orbits but also possess the potential to benefit the interplanetary exploration missions[5]. Therefore, developing novel approaches for orbital transfers and analyzing the characters is crucial and beneficial to the lunar exploration.

LFO is the circumlunar orbit, which possess constant mean eccentricity, mean orbital inclination, and mean argument of perilune[6]. As a special solution with constant parameters, LFO is broadly applied in some lunar exploration missions, such as the orbit for communication and navigation[7-8]. Besides, the LFO is an excellent option for relay satellite's mission orbit as well. LFO could be an alternative to the relay satellite's orbit to NRHO. Spacecraft on the LFO satisfies constraints and requirements for short-duration lunar dorsal relay support mission orbit [9]. Operating in the LFO, China's Queqiao-2 relay satellite provided support to the Chang'e-6 probe as it lifted off from the lunar surface, ensuring the success of the first mission to collect samples from the far side of the Moon. Placing relay satellites on LFO could not only improve communication coverage capability in the South Pole region of the Moon, but also reduce the fuel consumption for orbit maintenance. After completing relay communication, the satellite could stay on the LFO and update the software in orbit for adapting to new mission requirement in the future. Another choice is to transfer to other interesting orbits like NRHO.

Circular Restricted three-Body Problem (CR3BP) is usually used to simplify the real gravitation field of cislunar space. In CR3BP, the Halo orbit family is a series of periodic spatial orbits around the collinear Lagrange points, which can be regarded as a bifurcation of the Lyapunov orbit. NRHO is a subset of Halo orbits, which possess near-stable characteristics, named after its approximate straight-line shape. NRHO occupies an important location in the cislunar space. On the one hand, the appropriate distance from the Moon enables NRHO to be an outstanding orbit for detection and surveillance in the lunar vicinity[10]. On the other hand, the connectivity of NRHO makes it a transfer station in cislunar space and the launch platform to extraterrestrial celestial bodies[11]. Nowadays, the research related to NRHO has been extensively studied. One research area is to investigate the station-keeping problem for spacecraft on NRHO, which possesses both weak stability and important strategic value[12]. Some researchers are dedicated to finding novel approaches to directly determine ballistic multi-revolution quasi-NRHOs within the ephemeris model, which make the periodic orbits more practical in engineering significance[13]. Moreover, the orbital transfers connected with NRHOs are another research area of interest. For example, the transfer trajectory from NRHO to low-perilune orbits and even the lunar surface[14], and the transfers from an NRHO to a distant retrograde orbit[15]. The transfer strategies include direct transfer and transfer with the assistance of invariant manifold structure. These strategies each have their own advantages and disadvantages. The direct way will rapidly complete the transfer trajectory, while the manifold provides a fuel-saving possibility.

However, there is little research focusing on the design of transfer trajectories from LFO to NRHOs. The study on the transfer not only enriches the diversity of the lunar exploration mission but also provides novel investigation about the dynamical characteristic of LFO.

Therefore, this paper is intended to investigate the design of transfer trajectories from Sun-synchronized LFOs to NRHOs. The L2 southern 9:2 NRHO is selected as the research object in this paper. The contributions of this paper are as follows: Firstly, a novel multi-impulse transfer trajectory design method is proposed, which utilizes the stretching directions to accelerate the transfer time. The method transforms the trajectory design problem into a constrained nonlinear programming problem. In order to find the optimal solution, in other words the transfer with the minimum velocity increment, a global optimization is applied. Secondly, the proposed method is applied under both the CR3BP model and the high-fidelity model to design the transfer trajectories. Several transfer trajectories with different initial epochs are obtained and analyzed, which proved the effectiveness of the method.

The paper is organized as follows: in Section 1, the background information, including CR3BP and the calculation of NRHOs and LFOs are introduced. In Section 2, the transfer trajectory design method is described in detail. The results and relative discussion are in Section 3. Finally, the conclusions of the paper are discussed in Section 4.

1 Background

1.1 Lunar frozen orbit

There are several forms in the establishment of dynamic equations under the Earth-Moon system. To determine the description parameter of the lunar frozen orbit, the Moon-Centered Inertial at Epoch (MCIE) coordinate system is defined and utilized. Each epoch corresponds to unique states of the Earth and the Moon. Therefore, the definition of the system is different at different epochs. A coordinate system is defined with its origin at the lunar center of mass. The *x*-axis is directed from the Moon to the Earth, while the *z*-axis is parallel to the normal vector of the Moon's orbital plane. The *y*-axis is consequently defined by the right-hand rule. The coordinate system is shown in Fig 1.

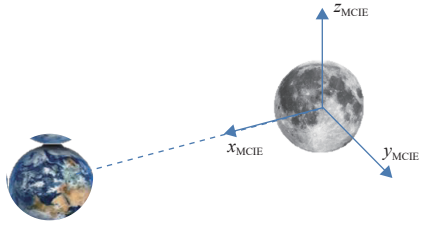


Fig. 1　Moon-Centered Inertial at Epoch (MCIE) coordinate system

Main perturbation to circumlunar orbit is Earth's third-body gravitation and the J_2 term of the Moon's gravitation. Therefore, the dynamic equations established in the MCIE coordinate system have to include the two main forces. The von Zeipel method[6] is used to obtain the system mean dynamics equation after double averaging, which is beneficial for simplifying problems. The equation is denoted using the Kepler orbital elements as follows[9]

$$\begin{cases} \dot{a} = \dot{a}_1 + \dot{a}_2 + \dot{a}_{J_2} \\ \dot{e} = \dot{e}_1 + \dot{e}_2 + \dot{e}_{J_2} \\ \dot{I} = \dot{I}_1 + \dot{I}_2 + \dot{I}_{J_2} \\ \dot{\Omega} = \dot{\Omega}_1 + \dot{\Omega}_2 + \dot{\Omega}_{J_2} \\ \dot{\omega} = \dot{\omega}_1 + \dot{\omega}_2 + \dot{\omega}_{J_2} \\ \dot{M} = \dot{M}_1 + \dot{M}_2 + \dot{M}_{J_2} \end{cases} \tag{1}$$

where a denotes the semi-major axis; e denotes eccentricity; I denotes orbital inclination; Ω denotes right ascension of ascending node; ω denotes argument of perilune; M is the mean anomaly. The subscript "1" refers to the first-order term of Earth's third-body gravitational effect; the subscript "2" indicates the second-order term of Earth's third-body gravitation; and the subscript "J_2" represents the second-degree zonal harmonic, which characterizes the Moon's non-spherical gravitational field. The expressions for these terms are as follows[9]

$$\begin{cases} \dot{a}_1 = 0 \\ \dot{e}_1 = \dfrac{15n_m^2}{16n\mu} e\sqrt{1-e^2}\sin^2 I \sin(2\omega) \\ \dot{I}_1 = \dfrac{15n_m^2}{16n\mu} \dfrac{e^2}{\sqrt{1-e^2}} \sin(2I)\sin(2\omega) \\ \dot{\Omega}_1 = \dfrac{3n_m^2}{8n\mu} \dfrac{\cos I}{\sqrt{1-e^2}} \left[-\left(2+3e^2\right)+5e^2\cos(2\omega)\right] \\ \dot{\omega}_1 = \dfrac{3n_m^2}{8n\mu} \dfrac{1}{\sqrt{1-e^2}} \left[\left(5\cos^2 I + e^2 - 1\right)+5(\sin^2 I - e^2)\cos(2\omega)\right] \\ \dot{M}_1 = \dfrac{3n_m^2}{8n\mu} \left[\left(3e^2+7\right)\left(3\cos^2 I - 1\right)+15(1+e^2)\sin^2 I\cos(2\omega)\right] \end{cases} \tag{2}$$

$$\begin{cases} \dot{a}_2 = 0 \\ \dot{e}_2 = \dfrac{135\mathrm{n}}{64\mu^2}\left(\dfrac{n_{\mathrm{m}}}{n_{\mathrm{m}}^*}\right)\left(\dfrac{n_{\mathrm{m}}}{n}\right)^3 e\left(1-e^2\right)\sin^2 I\cos I\sin(2\omega) \\ \dot{I}_2 = \dfrac{135n}{64\mu^2}\left(\dfrac{n_{\mathrm{m}}}{n_{\mathrm{m}}^*}\right)\left(\dfrac{n_{\mathrm{m}}}{n}\right)^3 e^2\sin I\cos^2 I\sin(2\omega) \\ \dot{\Omega}_2 = -\dfrac{9n}{128\mu^2}\left(\dfrac{n_{\mathrm{m}}}{n_{\mathrm{m}}^*}\right)\left(\dfrac{n_{\mathrm{m}}}{n}\right)^3 \left[2+33e^2-3(2-17e^2)\cos^2 I + 15e^2\left(1-3\cos^2 I\cos(2\omega)\right)\right] \\ \dot{\omega}_2 = \dfrac{27n}{64\mu^2}\left(\dfrac{n_{\mathrm{m}}}{n_{\mathrm{m}}^*}\right)\left(\dfrac{n_{\mathrm{m}}}{n}\right)^3 \cos I\left[11\left(1-e^2\right)+5\cos^2 I + 5\left(\sin^2 I - e^2\right)\cos(2\omega)\right] \\ \dot{M}_2 = -\dfrac{9n}{64\mu^2}\left(\dfrac{n_{\mathrm{m}}}{n_{\mathrm{m}}^*}\right)\left(\dfrac{n_{\mathrm{m}}}{n}\right)^3 \sqrt{1-e^2}\cos I\left[3\left(13+22e^2\right)+\left(11+34e^2\right)\cos^2 I + 15\left(1+2e^2\right)\sin^2 I\cos(2\omega)\right] \end{cases} \tag{3}$$

$$\begin{cases} \dot{a}_{J_2} = 0 \\ \dot{e}_{J_2} = 0 \\ \dot{I}_{J_2} = 0 \\ \dot{\Omega}_{J_2} = -\dfrac{3}{2}\dfrac{nr_{\mathrm{m}}^2 J_2}{a^2(1-e^2)^2}\cos I \\ \dot{\omega}_{J_2} = -\dfrac{3}{4}\dfrac{nr_{\mathrm{m}}^2 J_2}{a^2(1-e^2)^2}\left(1-5\cos^2 I\right) \\ \dot{M}_{J_2} = -\dfrac{3}{4}\dfrac{nr_{\mathrm{m}}^2 J_2}{a^2(1-e^2)^{3/2}}\left(1-3\cos^2 I\right) \end{cases} \tag{4}$$

where n denotes the average orbital angular velocity of the spacecraft around Moon; n_{m} refers to the average orbital

angular velocity of the Moon; n_{m}^{*} is the average autorotation velocity of the Moon; μ is the mass ratio coefficient of the Earth-Moon system, which is numerically equal to that in CR3BP; r_{m} is the physical radius of the Moon; $J_2 = 2.03 \times 10^{-4}$.

Lunar frozen orbit is defined as an orbit around the Moon in which the mean eccentricity, mean orbital inclination, and mean argument of perilune remain constant. In other words, it must satisfy the conditions required for a frozen orbit.

$$\begin{cases} \dot{e} = 0 \\ \dot{I} = 0 \\ \dot{\omega} = 0 \end{cases} \tag{5}$$

To satisfy the requirements for eccentricity, possible solutions can be derived from Eqs.(1)-(4), namely $e = 0$, $I = 0$ or $\sin 2\omega = 0$. Then the second frozen condition can be also satisfied simultaneously. The first two options impose overly restrictive constraints on the spacecraft's orbit. Consequently, in engineering applications, the solution $\sin 2\omega = 0$ is generally adopted, which allows the argument of perilune to be determined.

$$\omega = \pm\frac{\pi}{2} \tag{6}$$

Dynamic model can be further simplified. The new revision only includes the first-order term of Earth's third-body gravity, and the frozen condition can be rewritten as

$$\cos^2 I = \frac{3}{5}\left(1 - e^2\right) \tag{7}$$

Another requirement of the mission orbit is to synchronize the spacecraft with the Sun. Consequently, average angular velocity of the Sun's motion with respect to the Moon should be equal to the precession angular velocity of the Right Ascension of the Ascending Node (RAAN) of orbital plane. The combined impacts of third-body gravitational perturbation from the Earth and J_2 term disturbance from the lunar non-spherical gravitational field largely determine the orbital plane's precession. The RAAN's rate of change reflects this precession. Consequently, the RAAN precession rate must equal the Sun's relative angular velocity in order for the Sun to be synchronous:

$$\dot{\Omega} = \dot{\Omega}_1 + \dot{\Omega}_2 + \dot{\Omega}_{J_2} = n_{\mathrm{sun}} \tag{8}$$

where $n_{\mathrm{sun}} = 1.991\ 02$ rad/s is the average angular velocity of the Sun.

The Sun synchronous requirement may be reduced to the following when the Earth's third body gravitation's first order term is taken into account:

$$\dot{\Omega} = \frac{3}{4}\sqrt{\frac{3}{5}}\frac{n_{\mathrm{m}}^2}{n\mu}(1 + 4e^2) = n_{\mathrm{sun}} \tag{9}$$

Therefore, the eccentricity can be determined as

$$e^2 = \frac{1}{3}\sqrt{\frac{5}{3}}\frac{n\mu}{n_{\mathrm{m}}^2}n_{\mathrm{sun}} - \frac{1}{4} \tag{10}$$

The initial value of the lunar frozen orbit may be found using Eqs (7) and (10) respectively. The orbit's form may be ascertained if the orbital semi-major axis parameter is established. The spacecraft's phase should be as constant as possible to allow for easier monitoring and control on the ground. The definition of the nodal period is

$$T_{\mathrm{p}} = \frac{2\pi}{\dot{\omega} + \dot{M}} \tag{11}$$

The time it takes for a spacecraft on a disturbed elliptical orbit to make one full revolution around a central celestial body is known as the nodal period. Therefore, the spacecraft will be in the same phase for every measurement conducted by the ground station if the nodal period of the spacecraft is precisely adjusted to equal the measurement period. The restriction may be expressed as follows since the frozen condition forces the derivative of the argument of perilune to be zero:

$$\dot{M} = \dot{M}_1 + \dot{M}_2 + \dot{M}_{J_2} = \frac{2\pi}{T_R} \tag{12}$$

where T_R is the ground station measurement time. The final two terms might be disregarded for the purpose of calculating the beginning value. Eq (2) may be substituted into Eq (12) to obtain the starting value of n.

However, only the first-order term of the Earth's third-body gravity is considered in the dynamics to determine the initial value. The second-order term of the third-body gravity and the J_2 term of the Moon must also be considered in order to better meet the freezing and synchronization requirements in the high-fidelity model. Therefore, in the high-fidelity model, the orbital design problem is transferred to solve the non-linear equations.

$$\begin{cases}\dot{\Omega}=n_{\text{sun}}\\ \dot{\omega}=0\\ \dot{M}=2\pi/T_R\end{cases}\tag{13}$$

The differential correction approach can be used to solve the equations. The initial value needs to be established first. Then, using dynamic equations that incorporate the first-order term of the Earth's third-body perturbation, the simplified analytical partial derivative matrix is calculated. Lastly, the differential correction method is used to obtain high-fidelity numerical solutions in the full perturbation model that takes into account the non-spherical gravitational perturbation J_2 term of the Moon the first-order, and second-order terms of the Earth's third-body gravitational perturbation. The target variables and their values are given in Eq.(13), and the variables to be solved are $\boldsymbol{x}=[n, e, \cos I]^{\mathrm{T}}$.

The initial values and the converged results in the MCIE coordinate system are listed in Table 1.

Table 1　Initial values and the converged results

Orbital element	Initial value	Converged results
semimajor axis/km	10 003.061	9 931.320
eccentricity	0. 778 987	0.754 818
inclination/(°)	119.058	120.951

1.2　Circular restricted three-body problem

The CR3BP is a typical and reasonable approximation to describe the motion in the Earth-moon system. The spacecraft is considered as a mass point with negligible mass, which moves within the joint gravitation of Earth and Moon. Earth and Moon are primary and secondary celestial bodies, respectively. In this problem, Earth and Moon are assumed to move in a circle around their centroid. The motion of spacecraft is usually described in the synodic coordinate system shown as Fig 2. The origin is located at the barycenter of the Earth-Moon system, the x-axis pointing from Earth to the Moon, the z-axis pointing to the normal of the orbital plane, the y-axis meeting the right-hand rule with the other two axes. In order to simplify the computation, the non-dimensional equation is used to calculate the state of the spacecraft. The masses of Earth and the Moon are denoted as m_1 and m_2, respectively. The mass parameter is expressed as $\mu=m_2/(m_1+m_2)$. In this coordinate system, the Earth is at the fixed position$[-\mu, 0, 0]^{\mathrm{T}}$, and the Moon is located at$[1-\mu, 0, 0]^{\mathrm{T}}$ along the x-axis. The dynamic equations can be written as

$$\begin{cases}\ddot{x}-2\dot{y}=\dfrac{\partial\Omega}{\partial x}\\ \ddot{y}+2\dot{x}=\dfrac{\partial\Omega}{\partial y}\\ \ddot{z}=\dfrac{\partial\Omega}{\partial z}\end{cases}\tag{14}$$

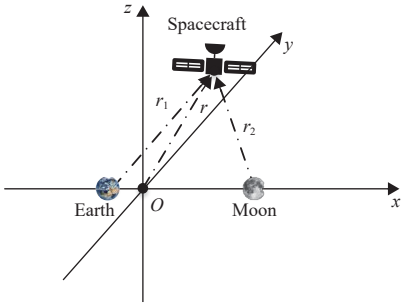


Fig. 2　Synodic coordinate system in the Earth-Moon CR3BP

where the effective potential is denoted by

$$\Omega=\frac{1}{2}\left(x^2+y^2\right)+\frac{1-\mu}{r_1}+\frac{\mu}{r_2}\tag{15}$$

The symbol r_1 and r_2 are respectively the distances from the spacecraft to Earth and Moon, which can be calculated by

$$\begin{cases}r_1=\sqrt{(x+\mu)^2+y^2+z^2}\\ r_2=\sqrt{(x-1+\mu)^2+y^2+z^2}\end{cases}\tag{16}$$

The physical parameters of the Earth–Moon system and the non-dimensional units are listed in Table 2.

Table 2　Physical parameters used in the dynamical model

Parameter	Value	Meaning
μ	$1.215\,058\,56\times10^{-2}$	Mass ratio of the Earth–Moon system
LU/km	$3.610\,248\,35\times10^{5}$	Length unit
TU/s	$3.414\,932\,35\times10^{5}$	Time unit
VU/(km·s^{-1})	1.057 194 68	Velocity unit

1.3　Near rectilinear Halo orbits in CR3BP

Halo orbits are one of the traditional forms of periodic orbits seen in the CR3BP. Studying the bifurcation of Lyapunov orbits will yield them. It is also possible to estimate the approximate initial value of Halo orbits analytically, from which the periodic orbit may be obtained using the differential correction approach[16]. The numerical continuation approach yields a single convergent solution for the whole Halo orbit family. The set of eigenvalues for

Halo orbits may be found in the monodromy matrix as follows: (1, 1, λ_1, $1/\lambda_1$, λ_2, $1/\lambda_2$). Orbital stability can be gauged using the stability indices. The eigenvalues of the monodromy matrix define stability indices

$$\nu_i = \frac{1}{2}\left(\|\lambda_i\| + \frac{1}{\|\lambda_i\|}\right) \tag{17}$$

where λ_i is the eigenvalues of the monodromy matrix.

The near rectilinear Halo orbits are a subset of Halo orbits whose projections in the x-z plane are approximately rectilinear. The NRHOs can be selected using the stability indices. Their stability indices values are generally between 1 and 2. The detailed selection of NRHOs can be found in the reference[16]. They are stable or near stable. Southern L_2 NRHOs are shown in Fig 3.

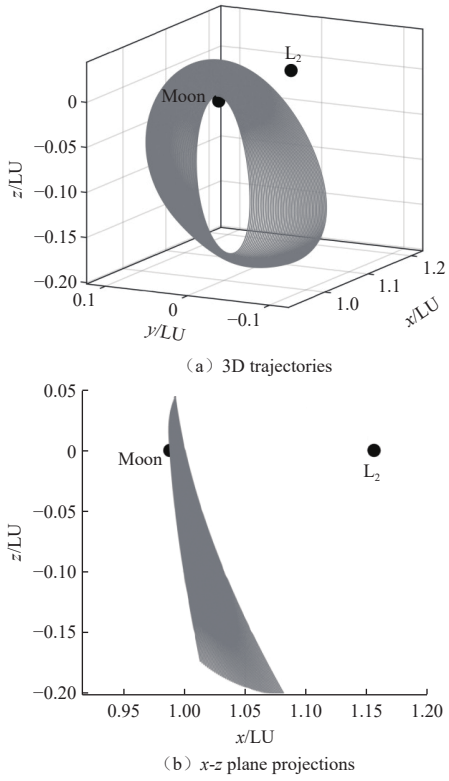


Fig. 3 Southern L2 NRHO

A synodic resonance occurs when the spacecraft's orbital period on an NRHO creates an integer ratio with the three-body system's synodic period. In particular, a p:q resonant NRHO indicates that the Moon completes q circles around Earth while the spacecraft completes p orbits in the NRHO. The southern L2 9:2 NRHO is chosen as the transfer's starting orbit in this investigation. Table 3 lists the selected NRHO's initial orbital characteristics.

Table 3 Initial orbital characteristics of 9:2 NRHO

x/LU	z/LU	v_y/VU	T/TU
1.021 881 3	–0.181 999 99	–0.102 950 79	1.509 263 5

The x, y, and v_y denote the corresponding state portions in synodic coordinate system. Other three state portions are zero. T is the period of NRHO in CR3BP.

Coordinate transformation between the Earth-centered inertial reference frame (ECI) and the Earth-Moon barycentric synodic reference frame can be found in reference [17] and [18]. The coordinate transformation between Earth-centered inertial reference frame and Moon-centered Inertial Reference Frame (MCI) can be directly achieved by addition and subtraction among vectors.

2 Multi-impulse transfer design method

Three impulses are involved in the proposed transfer trajectory method while leaving an LFO and entering an NRHO. The spacecraft's first separation from the LFO is intended to be initiated by the first impulse. This impulse plays the role in aiming the target position as well. The target position is determined by reversing calculation from NRHO. The last impulse is designed to exert on the NRHO along a special direction. Then the state of the spacecraft will be propagated backward along the time to obtain the aforementioned target point. The nominal second impulse is to fix the velocity difference at the target point. A nonlinear programming problem is used to formulate the overall trajectory design. To determine the least amount of velocity increment needed to execute the three moves, the transfer is optimized by a heuristic algorithm.

2.1 Transfer to NRHO using stretching directions

It is challenging to approach NRHOs using the invariant manifolds since they are close to stable periodic orbits. On the one hand, flying has a significant time expense. On the other hand, relying solely on invariant manifolds to significantly alter the spacecraft's state is challenging. Treating the leaving impulse as a three-dimensional optimization variable will increase the problem's nonlinearity and make it more challenging to solve.

The concept of stretching directions is proposed to assess the impact of a maneuver [19]. The spacecraft may

rapidly depart from the periodic orbit if there is a change in velocity in the direction of maximal stretching. The impact of initial variations on the terminal states is evaluated using the linear State Transition Matrix (STM).

$$\boldsymbol{\Phi}(t_f, t_0) = \frac{\partial x(t)}{\partial x_0} = \begin{bmatrix} \Phi_{r,r} & \Phi_{r,v} \\ \Phi_{v,r} & \Phi_{v,v} \end{bmatrix} \tag{18}$$

where t_0 and t_f are respectively, the initial time and final time; x_0 denotes the starting state; $x(t)$ denotes the final state at t_f. The STM can trace the influence of initial perturbation states on the deviation of terminal states. Consequently, it is possible to derive the modifications of the terminal states with the initial velocity perturbations that are specified.

$$\boldsymbol{\Phi}_{rv,v} = \begin{bmatrix} \Phi_{r,v} \\ \Phi_{v,v} \end{bmatrix} \tag{19}$$

where $\boldsymbol{\Phi}_{rv,v}$ is one 6 × 3 dimensional sub-matrix of $\boldsymbol{\Phi}(t_0, t_f)$. The changes of the terminal states can be regarded as the departure from the reference orbit. The effectiveness of the maneuver away from the beginning orbit is determined by how sensitive the final orbital state changes are to changes in the initial velocity. The magnitude of the maximal stretching σ that corresponds to the $\boldsymbol{\Phi}_{rv,v}$ can be used to map the sensitivity. The maximum stretching σ is derived from the eigenvalue of $\boldsymbol{\Phi}_{rv,v}$.

$$\sigma_i = \sqrt{\lambda_i} \tag{20}$$

where λ_i is the eigenvalue of the $\boldsymbol{\Phi}_{rv,v}$.

Carry out singular value decomposition to Eq. (19)

$$\boldsymbol{U}\Sigma\boldsymbol{V}^{\mathrm{H}} = \boldsymbol{\Phi}_{rv,v} \tag{21}$$

where Σ is a diagonal matrix combined with σ_i. $\boldsymbol{V}$ provides the direction information. Applying a velocity change along the component of $\boldsymbol{V}$ corresponding to the maximum σ_i, the states at the terminal moment takes the maximum change.

2.2 Design of the multi-impulse transfer trajectory

The design issue for the multi-impulse transfer trajectory is converted into a restricted nonlinear programming problem in this section. According to the chronological order, the first parameter to be designed is the state of the LFO before transfer. The frozen and Sun-synchronous conditions have determined three orbital elements. The other three orbital elements, Ω, ω, and M, are variables that need to be designed. Designing these parameters specially can satisfy the requirements of some missions, such as orientation towards the Sun. In this work, there is no extra requirement for the orbit, so the three parameters are all variable within appropriate ranges. The averaged orbital elements are required to transfer to osculating elements and the state vector can be obtained through osculating elements. At the end of the transfer process, the spacecraft will enter an NRHO. In CR3BP, the state on NRHO can be determined by a phase parameter, like the way of determining state on Kepler orbit using true anomaly. The phase parameter can also be replaced with time parameter, which is the method adopted in this work. From the perilune of the NRHO, the final state on the NRHO can be calculated by propagating forward for a flight time of $to\,f_0$. Then calculate the stretching direction of the terminal state and implement the maneuver along the stretching direction. Magnitude of the maneuver Δv_3 is one variable to be designed due to the direction of the vector having been determined by the proposed strategy, which reduces the dimension of variables from three to one. Following that, the state is propagated for tof_1 to drive the spacecraft away from NRHO in reverse along the time and reach some target position in the cislunar space. Lastly, the three-dimensional velocity increment $\Delta\boldsymbol{v}_1=[\,\Delta v_{1x}, \Delta v_{1y}, \Delta v_{1z}]^{\mathrm{T}}$ on LFO is implemented to aim the target position, and the spacecraft will fly tof_2 to arrive at the target position. Once positions are overlapped, another three-dimensional velocity $\Delta\boldsymbol{v}_2$ increment can be calculated using the two velocity vectors at the target position. To obtain the transfer trajectory with the minimum velocity increment, the global optimization is applied. The global design variables are

$$\boldsymbol{x}_G = [\ tof_0 \quad tof_1 \quad tof_2 \quad \Omega \quad \omega \quad M \quad \Delta v_3\ ] \tag{22}$$

In addition, another constrained local optimization problem is required to be nested in global optimization as follows

$$\boldsymbol{x}_L = [\ \Delta v_{1x} \quad \Delta v_{1y} \quad \Delta v_{1z}\ ] \tag{23}$$

The magnitude of velocity increments represents the local optimization objective, while the amount of the position difference serves as the constraint

$$\begin{aligned}&\text{Minimize: } y_L = f(\boldsymbol{x}_L) = \|\Delta \boldsymbol{v}_1\| \\ &\text{s.t. } \|\boldsymbol{r}_f - \boldsymbol{r}_t\| = 0\end{aligned} \tag{24}$$

where $\boldsymbol{r}_f$ is the position after spacecraft applied maneuver $\Delta \boldsymbol{v}_1$ and time of flight; $\boldsymbol{r}_t$ is the target position. By solve the local optimization problem, the transfer trajectory in multi-body dynamic model can be determined.

The global optimization objective is expressed as the sum of the magnitude of the velocity increments. The form is

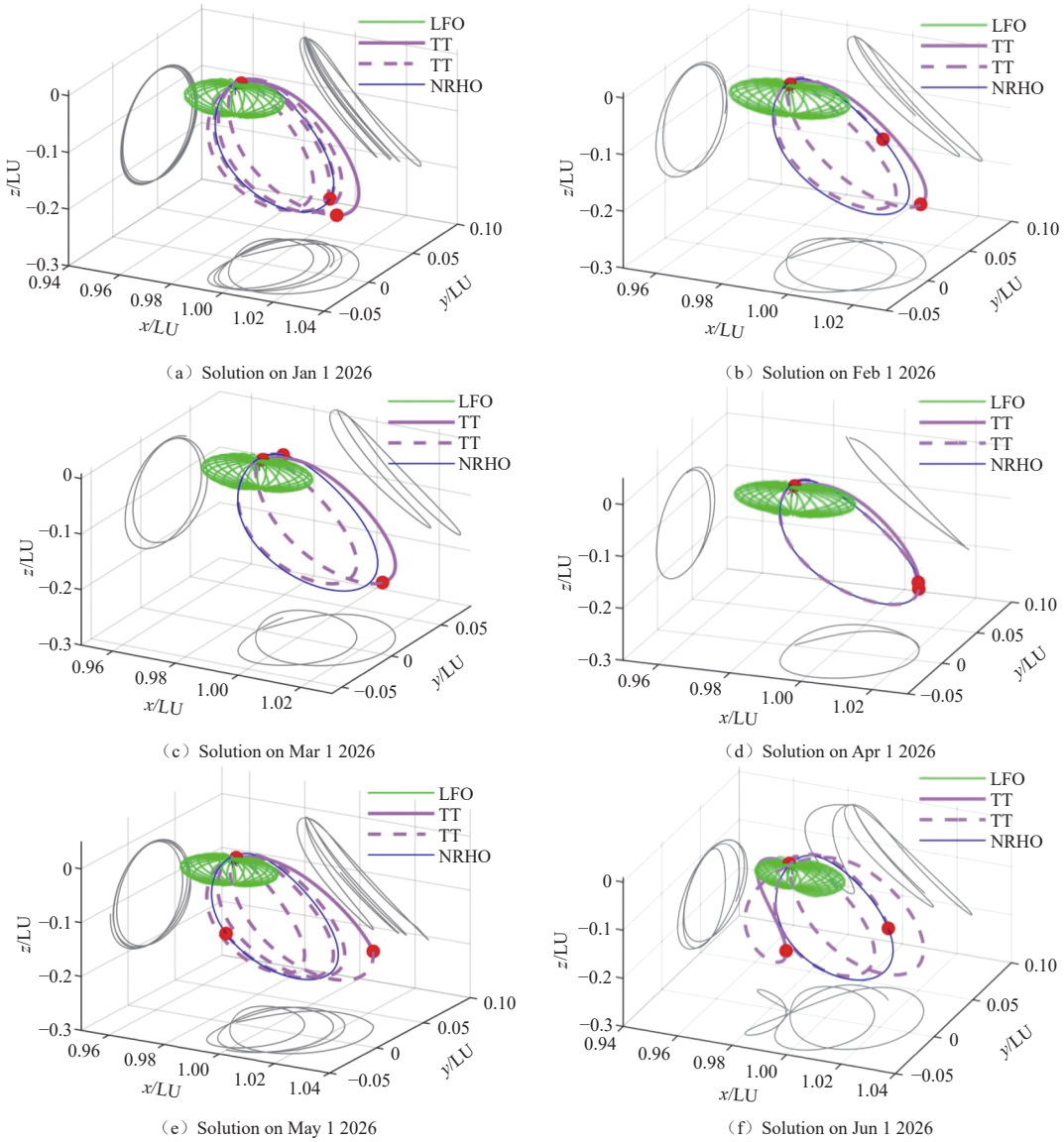
$$\text{Minimize: } y_G = \Delta v_3 + y_L + \|\boldsymbol{v}_f - \boldsymbol{v}_t\| \tag{25}$$

where $\boldsymbol{v}_f$ is the velocity of the corresponding state of $\boldsymbol{r}_f$; $\boldsymbol{v}_t$ is the velocity of the corresponding state of the $\boldsymbol{r}_t$. Heuristic algorithms like genetic algorithm can be used to solve the optimization problem.

3 Results and Discussion

3.1 Results in the CR3BP model

Several solutions of transfer trajectories in the CR3BP model are calculated by selecting several initial epochs through the algorithm in section 2. These solutions are shown in Fig 4. The three impulses are marked as red points, the transfer trajectory from LFO to NRHO is marked as purple solid and dashed lines, and it is referred to as “TT” in the legend. The projections on various planes are shown as solid gray lines. The detailed results are listed in Table 4.



（a）Solution on Jan 1 2026　（b）Solution on Feb 1 2026

（c）Solution on Mar 1 2026　（d）Solution on Apr 1 2026

（e）Solution on May 1 2026　（f）Solution on Jun 1 2026

Fig. 4　Transfer trajectories in the CR3BP

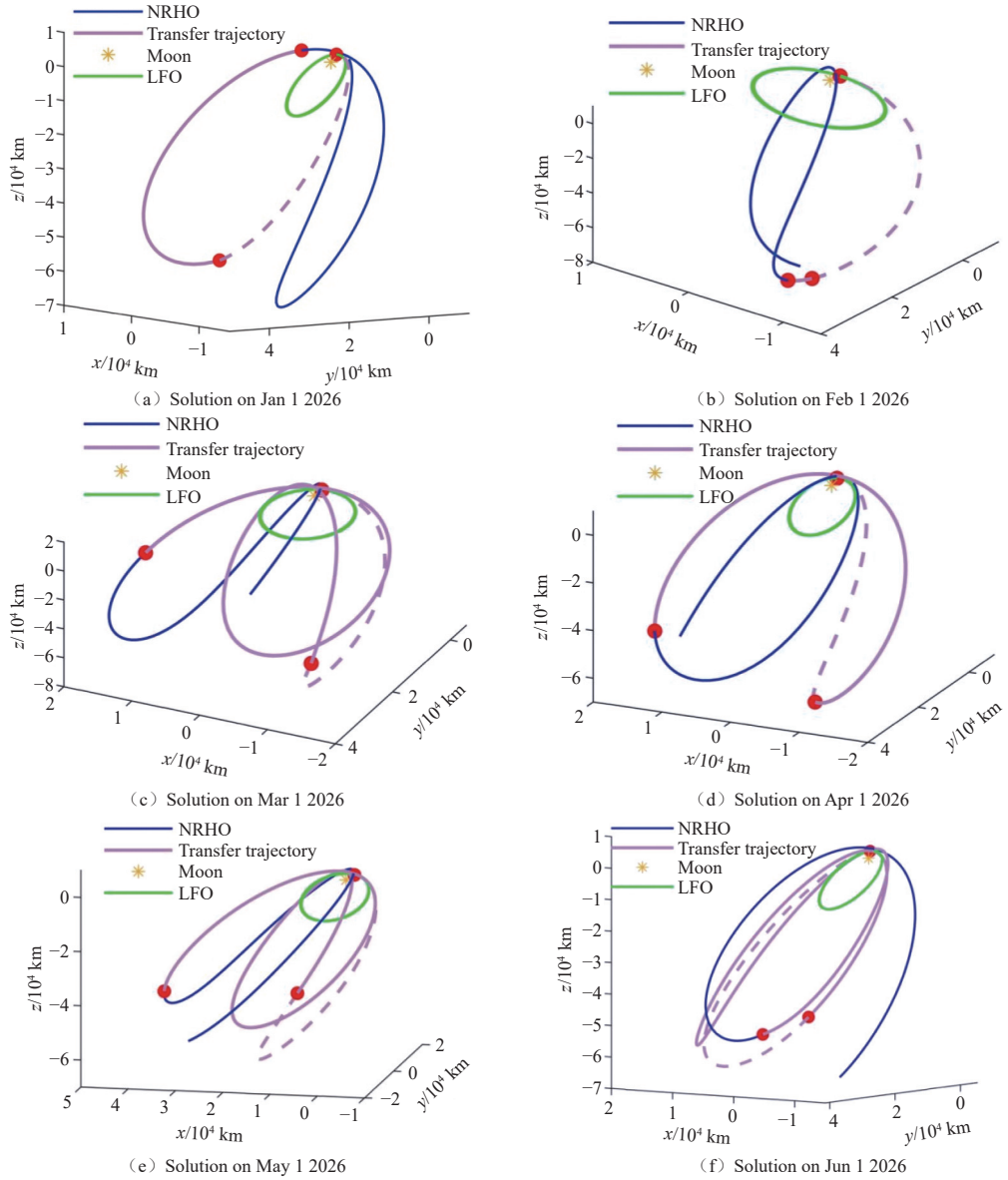
Table 4　Optimization results of cases for transfer trajectories in the CR3BP model with different epochs

Initial epoch	Total Δv/ ($m\cdot s^{-1}$)	Transfer time/d	1st Δv/ ($m\cdot s^{-1}$)	2nd Δv/ ($m\cdot s^{-1}$)	3rd Δv/ ($m\cdot s^{-1}$)
Jan 1 2026	120.22	26.49	99.83	17.96	2.43
Feb 1 2026	113.81	12.87	94.99	2.03	16.80
Mar 1 2026	110.54	12.90	101.29	3.08	6.17
Apr 1 2026	123.01	9.23	100.53	22.29	0.20
May 1 2026	127.41	26.65	104.82	18.62	3.97
Jun 1 2026	131.78	22.48	102.81	10.07	18.90

The departing point on LFO is similar in the first five solutions, but it is obviously different in the case on Jun 1 2026. The result is a local optimal solution, whose RAAN is different from the other solutions. That means the proper RAAN of LFO could reduce the transfer consumption to change the orbital plane. The detailed results show that the transfer time can be as short as less than 10 days and is usually less than one month. The most velocity increment is used to change the orbital energy, which shows the properness of the transfer method.

3.2　Results in the ephemeris model

The trajectories in the Moon-centered J2000 frame (MCI) are calculated under the dynamics considering the gravity of Earth, the Moon, the Sun, and Jupiter, which are as shown in Fig 5. The detailed results are listed in Table 5.



（a）Solution on Jan 1 2026　（b）Solution on Feb 1 2026

（c）Solution on Mar 1 2026　（d）Solution on Apr 1 2026

（e）Solution on May 1 2026　（f）Solution on Jun 1 2026

Fig. 5　Transfer trajectories in ephemeris model with different epochs

Table 5 Optimization results of cases

Initial epoch	Total Δv/（m·s^{-1}）	Transfer time/d	1st Δv/（m·s^{-1}）	2nd Δv/（m·s^{-1}）	3rd Δv/（m·s^{-1}）
Jan 1 2026	121.14	6.16	101.28	19.85	0.0082
Feb 1 2026	127.87	3.40	103.89	23.90	0.0700
Mar 1 2026	116.64	13.63	102.89	7.20	6.5400
Apr 1 2026	129.73	8.61	103.29	26.31	0.1200
May 1 2026	112.87	14.62	102.34	9.27	1.2400
Jun 1 2026	127.49	14.57	102.62	7.54	17.3100

Through optimization, six sets of transfer results are obtained near different initial epochs. The spacecraft may rapidly enter the terminal orbit with a small magnitude maneuver along the stretching direction since the third Δv values are less than 20 m/s, which is advantageous from the stretching direction.

By comparing the optimization results under two dynamic models, it can be concluded that the maneuver values are very close in magnitude. That means the fuel consumption of the proposed approach will not increase when considering more complex model. The actual position and velocity of the moon at different epochs will have an impact on the results of the two models.

4 Conclusions

An innovative multi-impulse transfer trajectory design approach from LFOs to NRHOs is proposed. The chosen research objects are the Sun-synchronized lunar frozen orbits and the 9:2 NRHO. Transfer flight time, LFO orbital parameters, and other optimization factors are used to build an optimization model for trajectory design. The transfer trajectories under the CR3BP and high-fidelity models are generated by solving this restricted nonlinear optimization problem as ideally as possible. Specifically, the proposed approach has the advantages of using the stretching direction technique to reduce the number of design variables while increasing orbital transfer efficiency. But it has the limitation on designing more complex transfer trajectories. With the suggested design approach, many trajectories are produced. With a velocity increment of only 110–140 m/s, detailed data demonstrate that transfers between the two orbits may be completed quickly. Trajectories designed under high-fidelity models have potential for engineering applications and can provide new mission orbit for future cislunar space missions.

References

[1] REN X Q，WU W R，WANG H Y，et al. Prospects of the lunar exploration development and key technologies[J]. Journal of Deep Space Exploration，2025，12(2)：99-109.

[2] SMITH M，CRAIG D，HERRMANN N，et al. The Artemis program：an overview of NASA's activities to return humans to the Moon[C]// Proceedings of 2020 IEEE Aerospace Conference. Big Sky，MT，USA：IEEE，2020.

[3] YUAN J C，HUANG Y D，LI P J，et al. Orbit determination for Chang'e-6 mission during the lunar orbit phase[J]. Advances in Space Research，2025，76(8)：4417-4429

[4] KANU N J，GUPTA E，VERMA G C. An insight into India's moon mission–Chandrayan-3：the first nation to land on the southernmost polar region of the Moon[J/OL]. Planetary and Space Science，2024，242：105864. https：//www.sciencedirect.com/science/article/pii/S003206332400028X.

[5] YANG H W，HU J C，BAI X L，et al. Review of trajectory design and optimization for Jovian system exploration[J]. Space：Science & Technology，2023(3)：1-14.

[6] NIE T，GURFIL P. Lunar frozen orbits revisited[J]. Celestial Mechanics and Dynamical Astronomy，2018，130(61)：1-35.

[7] ELY T A. Stable constellations of frozen elliptical inclined lunar orbits[J]. The Journal of the Astronautical Sciences，2020，53(3)：301-316.

[8] CHEN G Q，WU S H，YOU J H，et al. Communication-navigation integrated satellite constellation for lunar exploration：frozen-orbit-based hyinc walker[J]. IEEE Journal on Selected Areas in Communications，2024，42(5)：1436-1452.

[9] MENG Z F. Design of sun-synchronous and repeating tracking condition elliptical lunar frozen orbits[J]. Acta Aeronautica et Astronautica Sinica，2024，45(18)：1-16.

[10] TROFIMOV S，SHIROBOKOV M，TSELOUSOVA A，et al. Transfers from near-rectilinear halo orbits to low-perilune orbits and the Moon's surface[J]. Acta Astronautica，2020，167：260-271.

[11] RYAN W，ROLAND M. Options for staging orbits in cislunar space[C]//Proceedings of 2016 IEEE Aerospace Conference，Big Sky，MT，USA：IEEE，2016.

[12] GUZZETTI D，ZIMOVAN E M，HOWELL K C，et al. Stationkeeping analysis for spacecraft in lunar near rectilinear halo orbits[C]//Proceedings of 27th AAS/AIAA Space Flight Mechanics Meeting. San Antonio：AIAA，2017.

[13] LIU L，LIU Y. A note on the computation of multi-revolution NRHO under the ephemeris model[J]. Advances in Space Research，2025，75(3)：2889-2907.

[14] LU L，LI H Y，ZHOU W M，et al. Design and analysis of a direct transfer trajectory from a near rectilinear halo orbit to a low lunar orbit[J]. Advances in Space Research，2021，67(3)：1143-1154.

[15] OSHIMA K. The use of vertical instability of L1 and L2 planar Lyapunov orbits for transfers from near rectilinear halo orbits to planar distant retrograde orbits in the Earth–Moon system[J]. Celestial Mechanics and Dynamical Astronomy，2019，131(3)：1-28.

[16] ZIMOVAN-SPREEN E M，HOWELL K C，DAVIS D C. Near rectilinear halo orbits and nearby higher-period dynamical structures：

orbital stability and resonance properties[J]. Celestial Mechanics and Dynamical Astronomy，2020，132(5)：1-25.

[17] CANALES D，HOWELL K C，FANTINO E. Transfer design between neighborhoods of planetary moons in the circular restricted three-body problem：the Moon-to-Moon analytical transfer method[J]. Celestial Mechanics and Dynamical Astronomy，2021，133(8)：36.

[18] QIN L M，YANG H W，LI S. An efficient design method for long-term quasi-periodic near rectilinear halo orbits[J]. Journal of Astronautics，2024，45(1)：43-51.

[19] MURALIDHARAN V，HOWELL K C. Stretching directions in cislunar space：applications for departures and transfer design[J]. Astrodynamics，2023，7(2)：153-178.

The Author Profiles

LIANG Guoliang(2000−), male, PhD candidate, with research interests in astrodynamics, deep space exploration trajectory design and optimization.

Address: No.29, Jiangjun Road, Jiangning District, Nanjing University of Aeronautics and Astronautics (211106)

YANG Hongwei(1989−), male, Professor, with research interests in astrodynamics, deep space exploration trajectory design and optimization. **Corresponding author of this article**.

Address: No.29, Jiangjun Road, Jiangning District, Nanjing University of Aeronautics and Astronautics (211106)

E-mail: hongwei.yang@nuaa.edu.cn

月球冻结轨道至近直线晕轨道的转移轨道设计方法

梁国梁，杨洪伟

（南京航空航天大学 航天学院，南京 211106）

摘　要：针对月球冻结轨道与近直线晕轨道（Near Rectilinear Halo Orbit，NRHO）在地月空间探测中的重要战略意义，以及连接二者的转移轨道设计问题有待深入研究的现状，提出了一种从月球冻结轨道向L2点近直线晕轨道的多脉冲转移轨道设计方法，同时具备转移时间短和变轨机动量小的优点。通过最大拉伸方向理论确定了在NRHO的速度扰动方向，并将转移轨道设计问题建模为带约束的非线性优化问题，通过全局优化嵌套局部优化的方法，利用启发式算法进行优化求解，实现了航天器快速接近NRHO并以较小速度增量完成轨道插入。通过该方法得到了圆型限制性三体问题（Circular Restricted Three-Body Problem，CR3BP）模型和高精度模型下的转移轨道，为未来月球及深空探测任务中的转移轨道设计提供了有效的解决方案。

关键词：轨道设计与优化；月球冻结轨道；近直线晕轨道

[责任编辑：杨晓燕，英文审校：宋利辉]